Cell Reports, Volume *37*

Supplemental information

Corticospinal neuron subpopulation-specific developmental genes prospectively indicate mature segmentally specific axon projection targeting

Vibhu Sahni, Sara J. Shnider, Denis Jabaudon, Janet H.T. Song, Yasuhiro Itoh, Luciano C. Greig, and Jeffrey D. Macklis

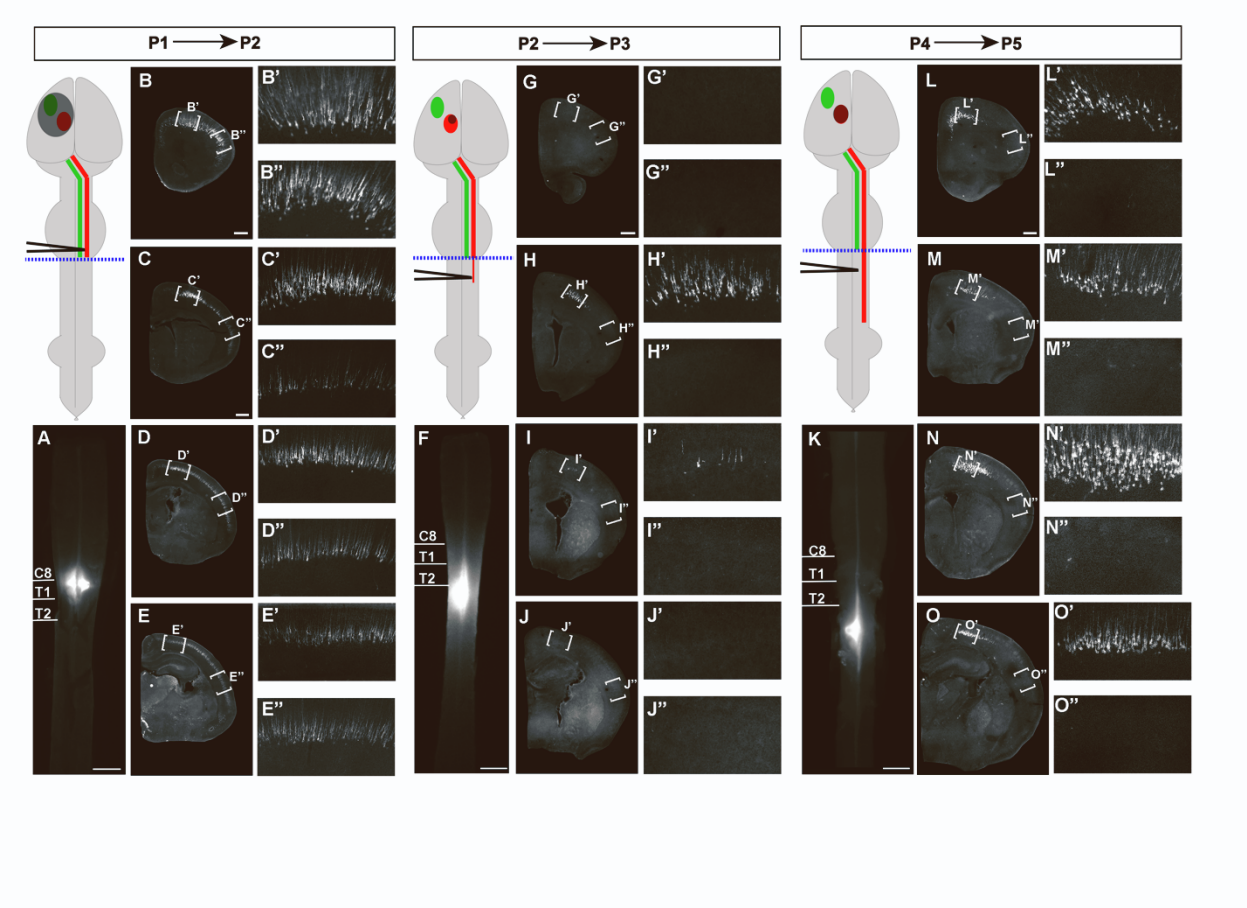

Figure S1: Differential CSN axon targeting past thoracic T2 by CSN_{BC} vs. CSN_{TL}.

Related to Figure 1

We investigated $CSN_{BC\text{-}lat}$ and CSN_{medial} axon extension from cervical C8, up to and past thoracic T2 (junction between cervical and thoracic cord indicated by dotted blue lines in schematics) during development by performing retrograde labeling (with CTB-555) at specific spinal segmental levels (black open triangles in schematics) at P1 (A-E"), P2 (F-J"), and P4 (K-O") to label CSN projecting axons to that spinal level at that time. (A) Whole mount image of the rostral spinal cord from a P2 mouse in which CTB-555 was injected into C8 at P1. (B-E) Coronal sections of the same P2 brain (from rostral to caudal) showing retrogradely labeled CSN. (B'-E") Magnification of boxed regions, showing medial (B'-E') versus lateral (B"-E") cortex; CSN in both medial and lateral cortex are labeled. (F) Whole mount image of a P3 rostral spinal cord in

which CTB-555 was injected into T2 at P2. (G-J) Coronal sections of the same P3 brain (from rostral to caudal) showing retrogradely labeled CSN. (G'-J") Magnification of boxed regions, showing medial versus lateral cortex. Retrogradely labeled CSN are seen only in rostral medial cortex (T', U') and not in lateral cortex (G"-J"). (K) Whole mount image of a P5 rostral spinal cord in which CTB-555 was injected into the rostral thoracic cord at P4. (L-O) Coronal sections of the same P5 brain (from rostral to caudal) showing retrogradely labeled CSN. (L'-O") Magnification of boxed regions, showing medial versus lateral cortex. Retrogradely labeled CSN reside in medial (L'-O') and not lateral (L"-O") cortex. Scale bars: (A, F, K) = 1mm; (B-E, G-J, L-O) =500μm. C8, cervical segment 8; T1, T2, thoracic segment 1, and 2.

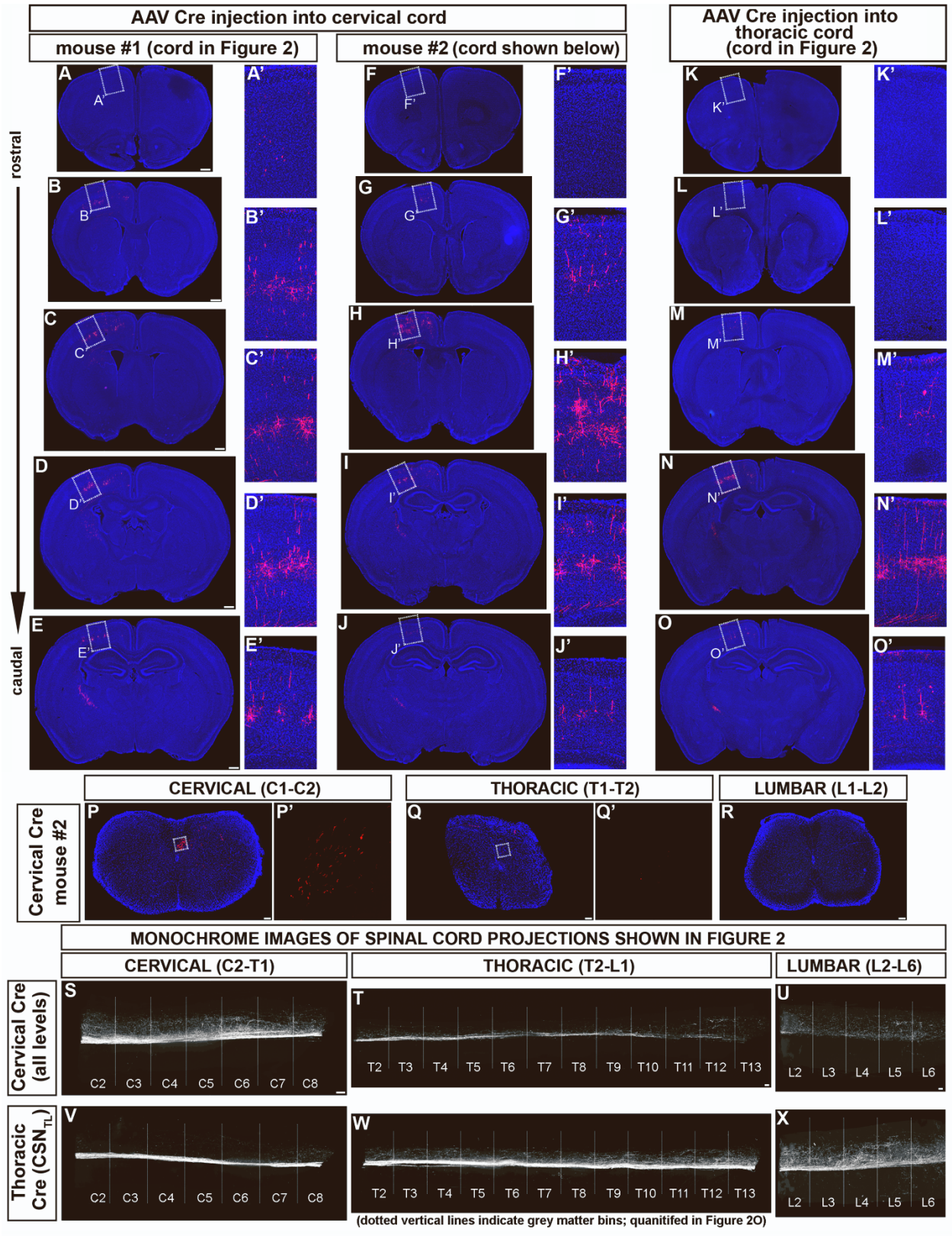
AAV Cre injection into cervical cord
mouse #1 (cord in Figure 2)
mouse #2 (cord shown below)
AAV Cre injection into thoracic cord (cord in Figure 2)
rostral
caudal
A
A'
B
B'
C
C'
D
D'
E
E'
F
F'
G
G'
H
H'
I
I'
J
J'
K
K'
L
L'
M
M'
N
N'
O
O'
Cervical Cre mouse #2
CERVICAL (C1-C2)
THORACIC (T1-T2)
LUMBAR (L1-L2)
P
P'
Q
Q'
R
MONOCHROME IMAGES OF SPINAL CORD PROJECTIONS SHOWN IN FIGURE 2
CERVICAL (C2-T1)
THORACIC (T2-L1)
LUMBAR (L2-L6)
Cervical Cre (all levels)
Thoracic Cre (CSN$_{TL}$)
S
T
U
V
W
X
C2 C3 C4 C5 C6 C7 C8
T2 T3 T4 T5 T6 T7 T8 T9 T10 T11 T12 T13
L2 L3 L4 L5 L6
(dotted vertical lines indicate grey matter bins; quanitifed in Figure 2O)

Figure S2. Intersectional viral labeling analyses identify that CSN subpopulations with segmentally distinct projections are spatially interdigitated in medial sensorimotor cortex. Related to Figure 3

Segmentally-specific CSN axon projections were investigated from development through maturation using intersectional viral labeling. As schematized in Figure 3, Cre-dependent AAV-CAG-FLEX-tdTomato was injected at P3 into medial sensorimotor cortex, followed by AAV-hsyn-EGFP-Cre injected at P4 in DF at either cervical C1 or thoracic T2. Mice were perfused at P28. (A-O) Coronal brain sections (from rostral to caudal) from mice injected with AAV-Cre into DF either at cervical C1 (A-J) or thoracic T2 (K-O). (A-E) Coronal brain sections from the same mouse (C1 AAV-Cre injected) whose spinal cord sections are shown in Figure 3 (Figure 3 B-D; I, K, M). (F-J) Coronal brain sections of a second C1 AAV-Cre injected mouse (mouse #2; indicated as outlier mouse in Figure 3O) in which nearly all (~98%) of tdTomato+ CSN axons terminate in cervical spinal cord. (K-O) Coronal brain sections from the same mouse (T2 AAV-Cre injected) whose spinal cord sections are shown in Figure 3 (Figure 3 F-H; J, L, N). (A'-O') Magnified views of the boxed regions in A-O, showing that labeled CSN reside in layer V, and that majority of CSN_{TL} labeled by thoracic T2 AAV-Cre reside in caudal sensorimotor cortex. (P-R) Axial sections of the spinal cord from mouse #2 ("outlier" in Figure 3O; injected with C1 AAV-Cre) at cervical (P), thoracic (Q), and lumbar (R) segments. (P', Q') High magnification single plane confocal images of DF (areas boxed in P, Q). Almost all (~98%) of tdTomato+ CSN axons present in cervical DF project only within the cervical cord, and do not extend to thoracic cord, indicating that virtually all CSN labeled in mouse #2 are $CSN_{BC\text{-}med}$. Notably, the cortical location of $CSN_{BC\text{-}med}$ labeled in mouse #2 are indistinguishable from locations of all CSN (both CSN_{TL} and $CSN_{BC\text{-}med}$) labeled in mouse #1, which includes both CSN_{BC} and CSN_{TL} (compare F-J' with A-E').

Further, the cortical location of the caudal subset of $CSN_{BC\text{-}med}$ labeled in mouse #2 is indistinguishable from CSN_{TL} labeled with thoracic T2 AAV-Cre (compare H-J' with M-O'). (S-X) Flattened 2D projections of digitally reconstructed P28 spinal cords from cervical (S, V), thoracic (T, W), and lumbar (U, X) spinal segments of mouse spinal cords injected with at P4 either cervical C1 AAV-Cre (S-U; monochrome images of the same mouse shown in Figure 3 I', K', M'; binning relates for Figure 3Q) or thoracic T2 AAV-Cre (V-X; monochrome images of the same mouse shown in Figure 3 J', L', N'; binning relates for Figure 3Q). Full 3D reconstructions of the same spinal cord from serially aligned horizontal sections are shown in Supplemental Videos 1-6. Scale bars: (A-O) = 500μm; (P-X) = 100μm.

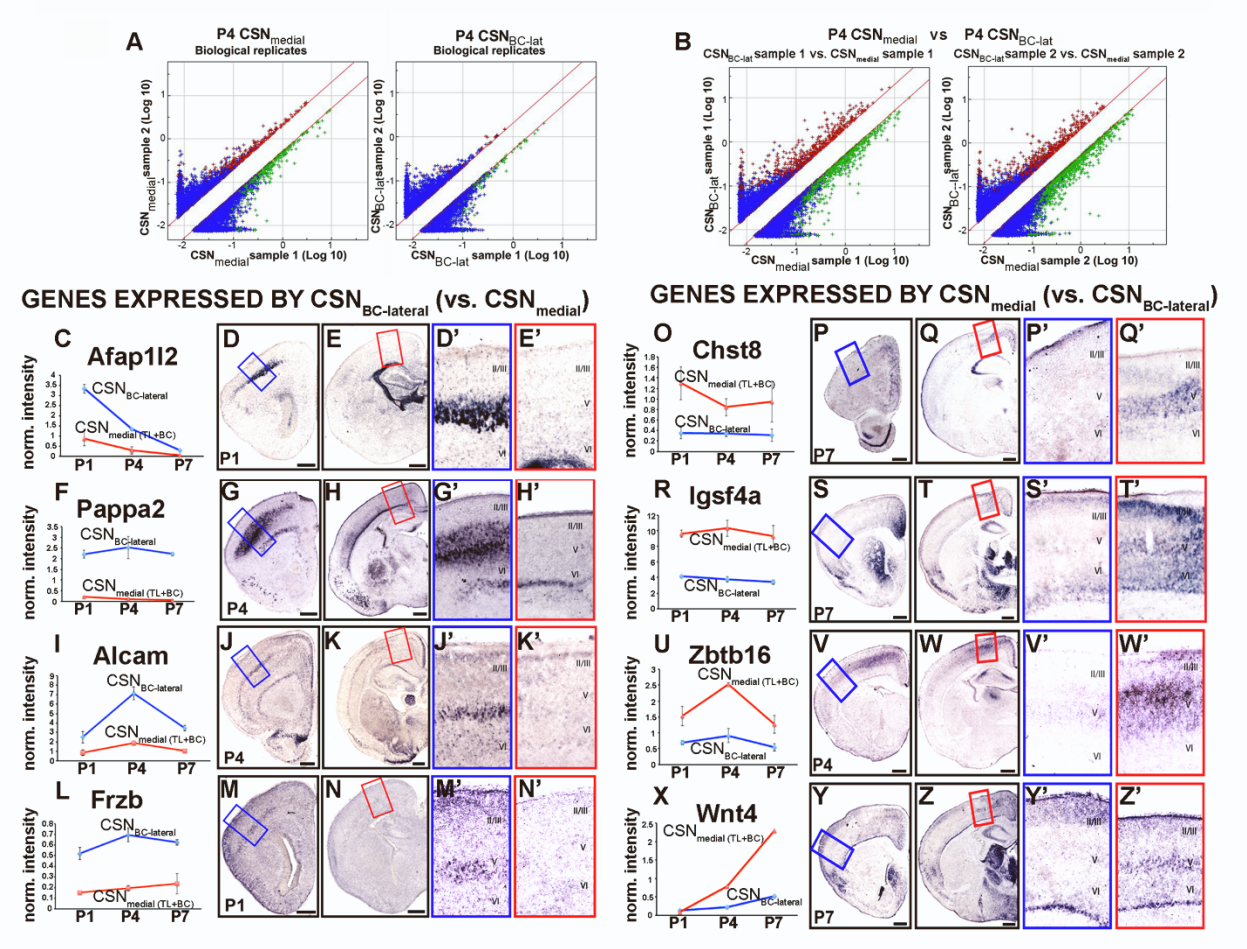

Figure S3. Potential molecular delineation of segmentally distinct CSN subpopulations identified by differential expression of a select number of genes.

Related to Figure 4

(A, B) Sample microarray intensity plots from P4 samples. All genes with ≥ 2-fold differential expression are shown. Genes that are not differentially expressed are shown in blue; differentially expressed genes (based on a p-value of less than 0.005) are shown in red and green, depending on population with enrichment. (A) Two plots of biological replicates of CSN_{medial} (left plot) and $CSN_{BC\text{-}latl}$ (right plot). Between CSN_{medial} replicates, only 441 transcripts out of >45,000 transcripts genes are "called" as differentially expressed. In biological replicates of $CSN_{BC\text{-}lat}$, only 95 genes are "called" as differentially expressed. (B) Plots showing differentially expressed genes between

CSN_{medial} vs. $CSN_{BC\text{-}lat}$ from two independent experimental replicates. >800 genes are differentially expressed between CSN_{medial} and $CSN_{lateral}$. Importantly, of these transcripts, only 65 are not replicated between in-parallel comparisons with biological replicates of either CSN_{medial} or $CSN_{BC\text{-}lat}$, supporting the reproducibility of the data. (C, F, I, L, O, R, U, X) Temporal profiles of gene expression from microarray data. (D, E, G, H, J, K, M, N, P, Q, S, T, V, W, Y, Z) *In situ* hybridization images for these genes on coronal brain section at ages indicated in the images. Not all genes are specific to layer V. (D', E', G', H', J', K', M', N', P', Q', S', T', V', W', Y', Z') Magnification of boxed regions showing rostrolateral versus caudomedial cortex. Even though some genes are expressed by other projection neuron populations, they are specific within layer V, with $CSN_{BC\text{-}lat}$-specific genes expressed in rostrolateral cortex and excluded from caudomedial cortex. Conversely CSN_{medial}-specific genes are only expressed within layer V in caudomedial cortex and excluded from rostrolateral cortex. Scale bars= 500 μm. II/III- VI, neocortical layers II/III -VI. Scale bars = 500μm.

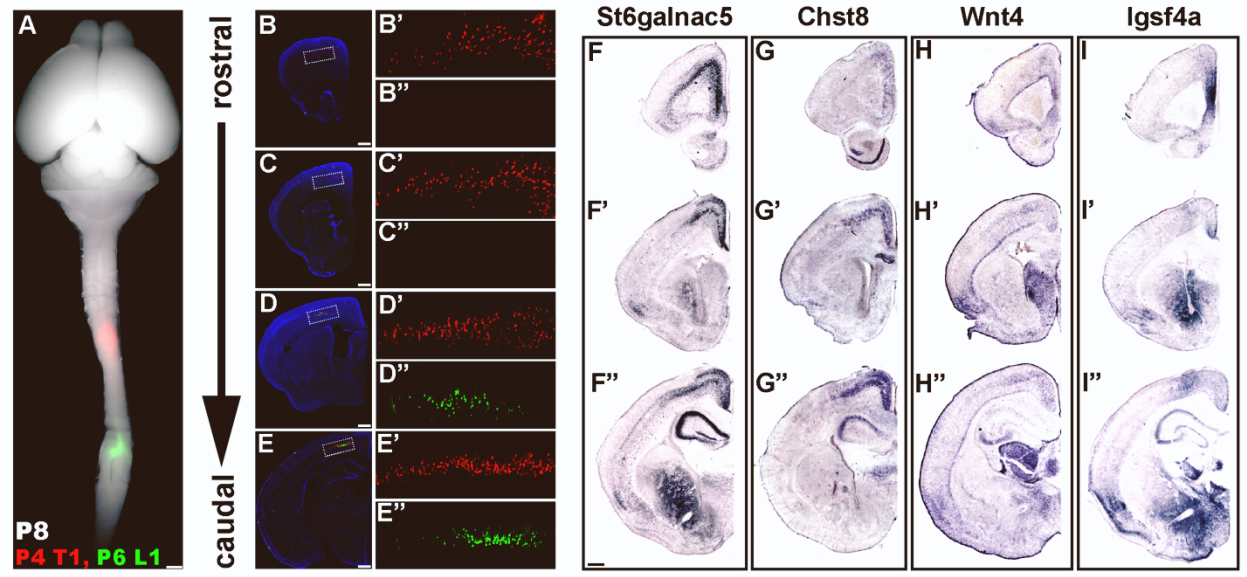

Figure S4. Additional CSN_{TL} segmental diversity correlates with spatial expression of select genes.

Related to Figure 4

(A) Whole mount image of a P8 mouse CNS showing injection sites of retrograde label CTB-555 (red) into thoracic T2 (at P4), and retrograde label CTB-647 (green) into lumbar L1 (at P6) DF. (B-E) Coronal sections of the same brain at four distinct rostro-caudal levels (same levels as shown and described in Figure1). (B'-E") Magnified views of regions boxed in B-E, demonstrating that CSN_{TL} reside throughout the rostro-caudal extent of medial sensorimotor cortex (red in B', C', D', E'), while lumbar-projecting CSN (CSN_L; green) are not present in rostral medial cortex (B", C"), and reside exclusively in caudomedial sensorimotor cortex (green in D", E"). (F-I") *In situ* hybridization images of displayed genes on coronal sections of a P7 brain from rostral (top) to caudal (bottom). *St6galnac5* is expressed throughout medial cortex (from rostral to caudal; F-F"); *Chst8* shows a gradient of expression from rostral to caudal, with lower expression in rostromedial and higher expression in caudomedial cortex (G - G"). *Igsf4a* and *Wnt4* are excluded from

rostromedial layer V (H, I), and are expressed only in caudomedial layer V (H', H", I', I"). Scale bars: (A) =1mm; (B-I") =500μm.

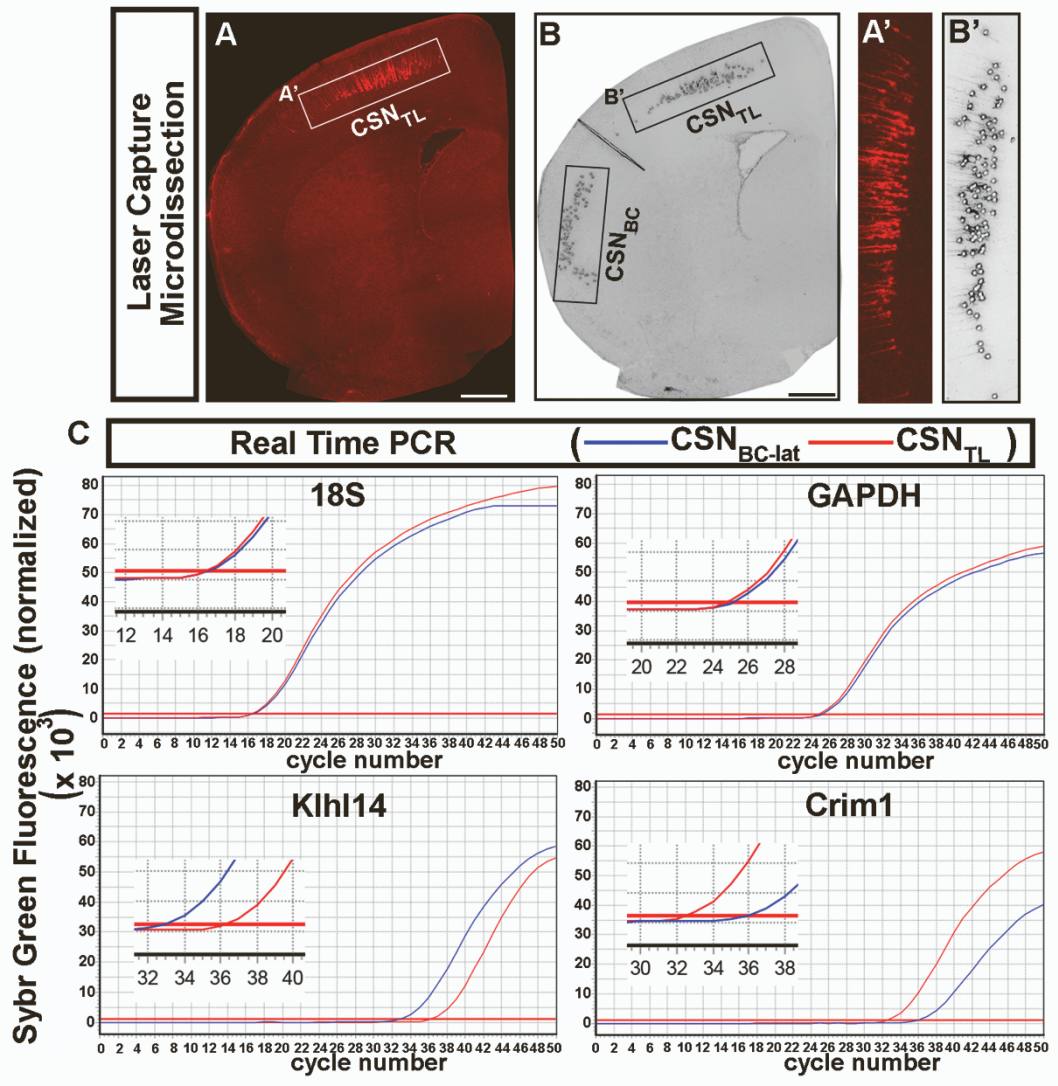

Figure S5: Laser capture microdissection and q-PCR confirms *Klhl14* and *Crim1* expression by $CSN_{BC\text{-}lat}$ versus CSN_{TL} during early development.

Related to Figure 5

(A-B) Additional confirmation of *Klhl14* and *Crim1* differential expression by laser capture microdissection and real time PCR. Retrogradely labeled CSN_{TL} in medial cortex (A) and high-level CTIP2+ neurons in lateral cortex were isolated from coronal brain sections using laser capture microdissection (B). (A', B') Magnification of boxed "CSN_{TL}" region in A, B showing pre- (A') and post- (B') laser capture of labeled CSN_{TL}. (C) Real time PCR performed on RNA

purified from captured neurons. Amplification plots (CSN_{TL} in red, $CSN_{BC\text{-}lat}$ in blue) measuring SyBr Green fluorescence for *18S*, *GAPDH* (loading controls), *Klhl14*, and *Crim1*. Insets show the magnified view of the section of the plots where the PCR amplification curves cross the threshold. *Klhl14* is expressed by $CSN_{BC\text{-}lat}$ (> 3-cycles higher than CSN_{TL}), while *Crim1* is expressed by CSN_{TL} (~2.5 cycles higher than $CSN_{BC\text{-}lat}$). Scale bar=500μm.

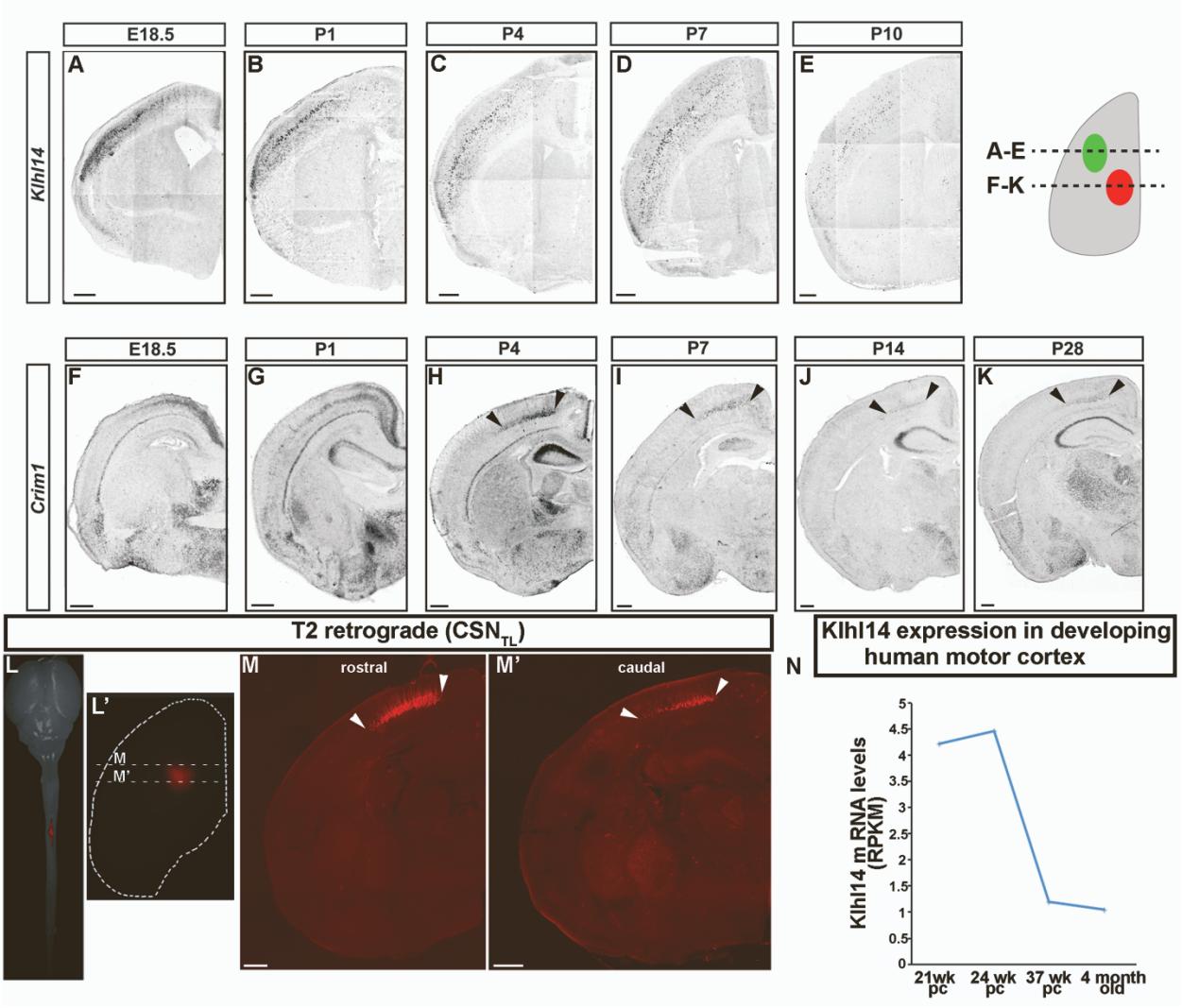

Figure S6. *Klhl14* and *Crim1* exhibit complementary expression in the developing neocortex, and their respective expression peaks at distinct developmental times.

Related to Figures 5 and 6

In situ hybridization images of *Klhl14* mRNA (A-E) and *Crim1* mRNA (F-K) on coronal sections of mouse brain at distinct developmental times. *Klhl14* is expressed in lateral neocortex and is excluded from medial cortex throughout development. In contrast, *Crim1* is specifically expressed in medial cortex, and is excluded from lateral cortex. *Klhl14* expression peaks early at E18.5 (A) and P1 (B). *Klhl14* expression then gradually declines from P4 (C) to P7 (D) to P10 (E). *Crim1* expression is present from E18.5 (F) and P1 (G). *Crim1* expression peaks at P4 (H), then declines

from P7 (I) to P14 (J) with CSN in P28 medial sensorimotor cortex expressing low *Crim1* levels (K). (L) Whole mount image of a P5 mouse CNS showing injection sites of CTB-555 (red) into thoracic DF at P4. (L') Whole mount fluorescent image of the same brain showing red fluorescence in medial sensorimotor cortex (i.e. CSN_{TL}). (M-M') Coronal sections of the same brain, at two distinct rostro-caudal levels (indicated by dotted lines in L'), demonstrate that, at both rostral (M) and caudal (M') levels, CSN_{TL} (red) reside almost exclusively in medial sensorimotor cortex (demarcated by white arrowheads). *Crim1* expression (F-K) in layer V occupies a similar domain in medial sensorimotor cortex (demarcated by black arrowheads). (N) Plot showing time course of *Klhl14* expression in the developing human motor cortex using RNA-seq data from obtained from the Allen Brain Atlas database (Miller et al., 2014). After 24 weeks (by which time the human CST has reached the caudal limit of the cervical cord), *Klhl14* levels sharply decline similar to developmental regulation and timing in mouse. Scale bars=400μm.

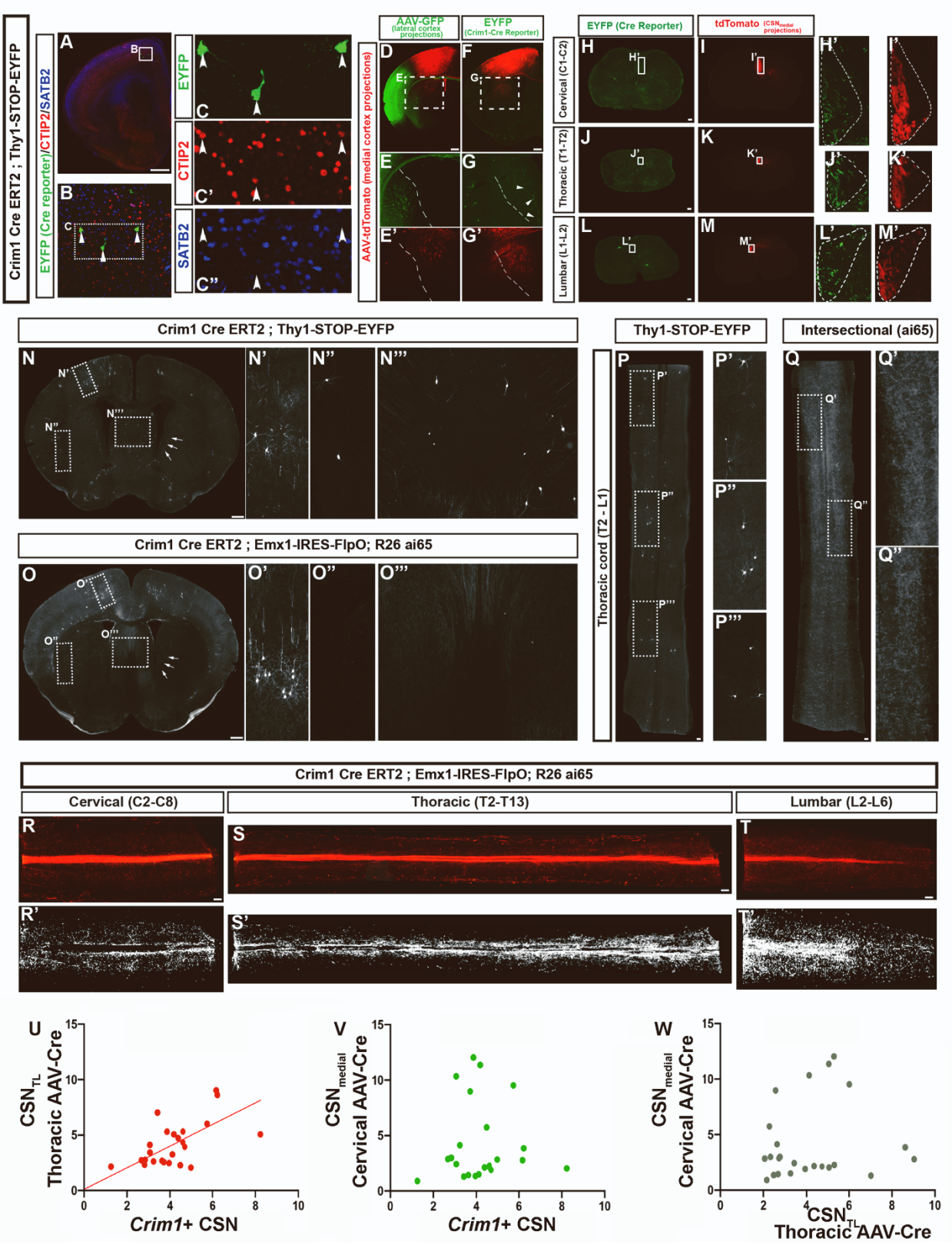
Crim1 Cre ERT2 ; Thy1-STOP-EYFP
EYFP (Cre reporter)/CTIP2/SATB2
EYFP
CTIP2
SATB2
AAV-GFP (lateral cortex projections)
EYFP (Crim1-Cre Reporter)
AAV-tdTomato (medial cortex projections)
EYFP (Cre Reporter)
tdTomato (CSN medial projections)
Cervical (C1-C2)
Thoracic (T1-T2)
Lumbar (L1-L2)
Crim1 Cre ERT2 ; Thy1-STOP-EYFP
Crim1 Cre ERT2 ; Emx1-IRES-FlpO; R26 ai65
Thy1-STOP-EYFP
Intersectional (ai65)
Thoracic cord (T2 - L1)
Crim1 Cre ERT2 ; Emx1-IRES-FlpO; R26 ai65
Cervical (C2-C8)
Thoracic (T2-T13)
Lumbar (L2-L6)
CSN TL Thoracic AAV-Cre
Crim1+ CSN
CSN medial Cervical AAV-Cre
Crim1+ CSN
CSN medial Cervical AAV-Cre
CSN TL Thoracic AAV-Cre

Figure S7. Crim1 expression in CSN during early development largely predicts thoraco-lumbar projection at maturity.

Related to Figure 7

(A-L) $Crim1^{GCE}$ mice were mated with Thy1-loxP-STOP-loxP-YFP (Thy1-STOP-YFP) mice to obtain double transgenic mice ($Crim1^{GCE}$; Thy1-STOP-YFP). We pulsed these mice with tamoxifen at P3.5 to induce Cre-mediated recombination in *Crim1*+ neurons, and utilized YFP reporter to investigate *Crim1*+ neurons, both molecular identity (at P5) and axonal projections (at P15). (A) Coronal section of a P5 $Crim1^{GCE}$; Thy1-STOP-YFP mouse brain labeled for YFP (green), CTIP2 (red), and SATB2 (blue). YFP+ neurons are located in layer V (high level CTIP2) in medial sensorimotor cortex, and excluded from lateral cortex. (B) Magnified view of the region boxed in (A), containing 3 YFP+ neurons (arrowheads). (C-C") Single confocal plane images demonstrating that all YFP+ neurons (arrowheads in C-C") in medial cortex are CTIP2-positive (C') and SATB2-negative (C"). (D) Coronal section of a P15 WT mouse brain injected with AAV-EGFP (green) in lateral cortex ($CSN_{BC\text{-}lat}$) and AAV-tdTomato (red) in medial cortex (CSN_{medial}) at P0 (similar to Figure 1). (E-E') Magnified view of region boxed in (D) in the striatum, showing the internal capsule. $CSN_{BC\text{-}lat}$ axons (green) course laterally in the internal capsule, while CSN_{medial} axons course medially (red) (dashed line demarcates the approximate boundary between $CSN_{BC\text{-}lat}$ and CSN_{medial} axons). (F) Coronal section of a $Crim1^{GCE}$; Thy1-STOP-YFP double transgenic mouse brain at P15 that was injected with AAV-tdTomato in medial cortex at P0, then pulsed with tamoxifen at P3.5 (G-G'). Magnified view of region boxed in (F), showing the internal capsule where most *Crim1*+ CSN axons (green) traverse medially (arrows in G), co-localized with anterogradely labeled CSN_{medial} axons (red in G'). (H-M) Axial sections of the spinal cord from the same mouse as in F-G', at cervical C1-C2 (H, I), thoracic T1-T2 (J, K), and lumbar L1-L2 (L,

M). *Crim1*+ CSN axons are seen in DF (green in H, J, L) co-localized with anterogradely labeled CSN_{medial} axons (labeled by AAV-tdTomato injection in medial sensorimotor cortex; red in I, K, M). (H'-M') Magnified views of the regions boxed in H-M, displaying *Crim1*+ axons in DF. Dashed outline demarcates the region of DF traversed by anterogradely labeled CSN_{medial} axons (Quantification of axon extension by these *Crim1*+ CSN axons is shown in Figure 7 F). (N) Coronal brain section of a P15 $Crim1^{GCE}$; Thy1-STOP-YFP mouse that was pulsed with tamoxifen at P3.5, showing YFP + CSN in medial cortex (N'). In addition, YFP+ neurons are seen in the striatum (N") and medial septum (N'''), consistent with *Crim1* expression (expression detailed in Main Figures 5, 6, and 7, as well as Figures S5, and S6). (O) Coronal brain section of a P24 $Crim1^{GCE}$; Emx1-IRES-FlpO; ai65 intersectional reporter mouse (CERai65 as schematized in Figure 7B) that was pulsed with tamoxifen at P3.5 in which tdTomato+ (*Crim1*+) CSN are present in medial cortex (O'). Using this intersectional system, there is no non-CSN neuronal labeling observed in the striatum (O") or the medial septum (O'''). (P) Horizontal section of the thoracic spinal cord from a P15 $Crim1^{GCE}$; Thy1-STOP-YFP mouse that was pulsed with tamoxifen at P3.5, in which YFP+ spinal neurons are present in the spinal gray matter. (P', P", P''') Magnified views of boxed regions in P. (Q) Horizontal section of the thoracic spinal cord from a P24 CERai65 intersectional mouse that was pulsed with tamoxifen at P3.5. (Q', Q") Magnified views of boxed regions in Q, showing only CSN axon collaterals without any spinal neuronal labeling. (R-T') Flattened 2D projections of digitally reconstructed spinal cords from a CERai65 intersectional mouse that was pulsed with tamoxifen at P3.5 (same mouse shown in O, Q). Projections of the entire rostro-caudal extent of the cervical C2-C8 (R, R'), thoracic T2-T13 (S, S'), and lumbar L2-L6 (T, T') spinal segments of this mouse are shown (monochrome hemisections from these images are presented in Main Figure 7N, O, P for direct comparison with CSN_{medial} and CSN_{TL} axons).

(R'- T') Same image as in (R-T) edited to remove main CST axons in DF, showing only the tdTomato+ CSN axon collaterals in spinal gray matter. (U) Pearson correlation comparing axon collateral distribution at each spinal segmental bin between *Crim1*+ axons (in CERai65 genetic intersectional mice) and CSN_{TL} axons identified using intersectional viral labeling with AAV-Cre at thoracic T2. There is significant correlation between the groups ($p<0.003$). (V) Pearson correlation comparing axon collateral distribution at each spinal segmental bin between *Crim1*+ axons (in CERai65 genetic intersectional mice) and CSN_{medial} axons identified using intersectional viral labeling with AAV-Cre at cervical C1. There is not correlation between the groups. (W) Pearson correlation comparing axon collateral distribution at each spinal segmental bin between CSN_{TL} axons identified using intersectional viral labeling with AAV-Cre at thoracic T2 and CSN_{medial} axons identified using intersectional viral labeling with AAV-Cre at cervical C1. There is not correlation between the groups. Scale bars: (A, D-G', N, O) = 500μm; (H-M, P-T) = 100μm.

GENES EXPRESSED BY $CSN_{BC\text{-}lat}$

Identity (potentially regulating multiple aspects of $CSN_{BC\text{-}lat}$ development)

Frzb	Frizzled-related protein	NM_011356
Pappa2	pappalysin 2	NM_001085376.2
Postn	Periostin; osteoblast specific factor	NM_015784
Edil3	Del1, EGF-like repeats and discoidin I-like domains 3	NM_001037987
Cldn16	Claudin 16; paracellin1 (PCLN1; tight junction protein)	NM_053241
Lce1i	riken cDNA 2310069N01, late cornified envelope 1	NM_029667

Early (potentially regulating $CSN_{BC\text{-}lat}$ axon extension)

Klhl14	Kelch-like 14	NM_001081403
Ermin	Galnt5, riken cDNA A330104H05	NM_029972
Afap1l2	Actin filament associated protein1-like 2	NM_146102
Dbp	D site albumin promoter binding protein	NM_016974
Ror-β	RAR-related orphan receptor beta	NM_001043354
Cdh4	Cadherin 4	NM_009867

Intermediate/Late (potentially regulating later aspects of $CSN_{BC\text{-}lat}$ axonal collateralization and connectivity)

Cartpt	CART (Cocaine- and amphetamine- regulated transcript) prepropeptide	NM_001081493
Alcam	Activated leukocyte cell adhesion molecule	NM_009655
Laptm4b	Lysosomal-associated protein transmembrane 4B	NM_033521
Pdlim5	PDZ- and LIM domain 5	NM_019808
Lum	Lumican; Keratan Sulfate Proteoglycan	NM_008524
Fxyd7	FXYD domain-containing ion transport regulator 7	NM_022007

GENES EXPRESSED BY CSN_{medial}

Identity (potentially regulating multiple aspects of $CSN_{BC\text{-}med}$ and CSN_{TL} development)

Chst8	Carbohydrate (N-acetylgalactosamine 4-0) sulfotransferase 8	NM_175140
Igsf4a	Immunoglobulin superfamily, member 4A; involved in cell-adhesion	NM_001025600
Crymu	Mu-crystallin	NM_016669
Etv1	Ets variant gene 1, ER81	NM_007960
Odz4	Odd Oz/ten-m homolog 4	NM_011858
Dact1	Dapper homolog 1, antagonist of beta-catenin	NM_021532
Slc16a2	solute carrier family 16 (monocaboxylic acid transporters), member 2	NM_009197

Early (potentially regulating CSN_{TL} axon extension)

Crim1	Cysteine rich transmembrane BMP regulator 1 (chordin like)	NM_015800
Zbtb16	Zinc finger and BTB domain containing 16	NM_001033324
Prokr2	Prokineticin receptor 2	NM_144944
Odz2	Odd Oz/ten-m homolog 2	NM_011856
Cav1	Caveolin 1	NM_007616
Tshz2	Teashirt zinc finger family member 2	NM_080455
Cntn4	Contactin 4	NM_173004
Runx1t1	Runt-related transcription factor 1	NM_001111026

Intermediate/Late (potentially regulating later aspects of CSN_{medial} axonal collateralization and connectivity)

St6galnac5	ST6(alpha-N-acetyl-neuraminyl-2,3-beta-galactosyl-1,3)-N-acetylgalactosaminide alpha-2,6-sialyltransferase 5	NM_012028
Wnt4	Wingless-related MMTV integration site 4	NM_009523
Cbln1	Cerebellin 1	NM_019626
Zcchc12	Zinc finger, CHCC domain containing 12	NM_028325
Ntng1	Netrin G1	NM_001163349
Htr2c	5-hydroxytryptamine (serotonin) receptor 2C, 5HT1c, Htr1c	NM_008312
Gpc5	Glypican 5	NM_175500

Table S1. (Related to Figure 4, Figure S3, Figure S4).

$CSN_{BC\text{-}lat}$ and CSN_{medial}-specific genes categorized by the time course of differential expression by distinct subpopulations.

***IN SITU* HYBRIDIZATION PROBES**				
Gene Name	**Source**	**Forward Primer (5' – 3')**	**Reverse Primer (5' – 3')**	**Probe Size (bp)**
Afap1l2	ABA	GGAAGTCACGCTGGTGCT	GCCTCTCCTTCTCCTCCG	935
Alcam	ABA	GCAGCCTGTGGAAGGAGA	CACTGCCGGTAATGGTCC	826
Cartpt	ABA	GCTACCTTTGCTGGGTGC	CAACAGGGAAAGAGCCCA	470
Crim1	RT-PCR	TCTTATCTGCAAGTGCCGAGAGGTCCCTC	TCACACCGTTTGGTAGAAGTTGTCTGCC	1354
Crymu	Arlotta et. al. (2005)	ACTGGCGAGAACTGGATGAC	GCCATCACCCCTTAACAGAA	436
Chst8	ABA	CCCCAGCATGATAGCCAC	CGGCTAACATGGTCCCAG	817
Ermin	RT-PCR	GAGACCCAGGCATACTACAAGG	GCTCTGTGACAATGCTTACCTG	985
Frzb	ABA	TCTCTCCTGAGGCCATCG	TGCATTCTCAATCGGGGT	853
Igsf4a	ABA	GCAGACCATTTACTTCAGGGAC	CAGAATGATGAGCAAGCATAGC	943
Klhl14	genepaint	GTTCGCAACTCAGATCACACTC	GGCAGAGAACAATTGCCAAAG	451
Pappa2	genepaint	TCCCTTGGCTCCAGTATTTGAAG	CAGCCCCTTTCACTGTGTTTGC	474
St6galnac5	ABA	CTATGGGCTTGACGTGGG	TGCTCCCGGTTCAGTTTC	901
Wnt4	ABA	CAGCATCTCCGAAGAGGAGAC	GCTTTAGATGTCTTGTTGCACG	749
Zbtb16	RT-PCR	ATGAAAACATACGGGTGTGAA	CCAAGGCCAAGTAACTATCAGG	908
GENOTYPING				
Mouse line	**Source**	**Forward Primer (5' – 3')**	**Reverse Primer (5' – 3')**	
Crim1^{GCE} (Cre allele)	Jackson Labs	GCGGTCTGGCAGTAAAAACTATC (oIMR 1084)	GTGAAACAGCATTGCTGTCACTT (oIMR 1085)	
Thy1-STOP-YFP mice	Jackson Labs	AAGTTCATCTGCACCACCG (oIMR0872)	TCCTTGAAGAAGATGGTGCG (oIMR1416)	
Ai65D (WT allele)	Jackson Labs	AAGGGAGCTGCAGTGGAGTA (oIMR9020)	CCGAAAATCTGTGGGAAGTC (oIMR9021)	
Ai65D (mutant allele)	Jackson Labs	GGCATTAAAGCAGCGTATCC (oIMR9103)	CTGTTCCTGTACGGCATGG (oIMR9105)	
Emx1-IRES-FlpO (WT allele)	This paper	GAAGGGTTCCCACCATATCAACC	CATAGGGAAGGGGGACATGAGAG	
Emx1-IRES-FlpO (FlpO allele)	This paper	GAAGGGTTCCCACCATATCAACC	AACTCCCAGGCGGGGATCAG	
qPCR				
Gene Name	**Source**	**Forward Primer (5' – 3')**	**Reverse Primer (5' – 3')**	
GAPDH	This paper	GTCGTGGATCTGACGTGCC	TGCCTGCTTCACCACCTT	
18S	This paper	AACCCGTTGAACCCCATT	CCATCCAATCGGTAGTAGCG	
Klhl14	This paper	TGACGACAGCATTTATCTAGTTGGAGGA	AACTCGAAGGTGATGTGGCTG AAC	
Crim1	This paper	AGGAGAAGGACTGCGTTTATG	ATCGGTGAGGAAGCCAAAG	

Table S4.

Primer sequences used in this study.